

Project Title:

**Numerical study on new functionality of spin-heat cross effect**

Name: ○Qinfang Zhang

Laboratory at RIKEN: Computational Condensed Matter Physics Lab.

**Introduction**

Stimulated by miraculous properties of graphene, scientists show great interests in other two dimensional (2D) monolayer materials, such as silicene, h-BN and boron sheet. Among them, silicene, a silicon film of one atomic thickness as the counterpart of graphene, has been theoretically predicted and experimentally synthesized on Ag(111), Ir(111), and ZrB<sub>2</sub>(0001) substrates recently. Different from the flat honeycomb lattice of graphene, silicene has to be stabilized by a low buckling of about 0.44 Å as predicted by density functional theory (DFT) calculations. Most importantly, silicene resembles the unique linear Dirac cone of graphene; thus massless fermions in silicene possess ultrahigh Fermi velocity of about 10<sup>6</sup> m/s, comparable to that of graphene. Such unique electronic property of silicene sheet can be either retained or tailored when it is supported on semiconducting BN and SiC substrates. Moreover, integration of silicene into microelectronic devices is very tempting since it may be compatible with the mature silicon-based semiconductor technology.

To date, although the free-standing silicene sheets have not been isolated yet, silicene is believed to have a bright future and the relevant studies are in the stage of booming development in vigor. It is thus urgent to theoretically explore the structure, stability and physical properties of free-standing silicene in advance. Among those fundamental issues, defects are crucial for production and future applications of silicene monolayer materials. Previous results showed that most of the outstanding properties of silicene and graphene rely on the defect-free perfect structures. Even though the formation energies of defects in graphene are rather high (e.g., ~7.5 eV for a single vacancy), there is a cornucopia of reports on the defects in graphene from both experimental observations and theoretical calculations. Naturally, one expect certain amount of defects must also exist in silicene, and some distinct structural defects were actually found in the STM images from recent experiments.

In the fabrication of two-dimensional films, the most commonly found defects are grain boundaries, which might be avoided by further improving the growth technique. However, for the purpose of characterization and device applications, the as-prepared 2D films are usually exposed under high-energy irradiations of laser, electrons, and ions, which would certainly induce local point defects, such as Stone-Wales rotation, single and double vacancies (abbreviated as SW, SV and DV,

respectively, hereafter). It is conceivable that the intrinsic properties of these monolayer sheets might be remarkably altered once certain amount of defects were generated. In the case of graphene, SV defect and C adatom will result in local magnetic moments. Chen et al. have observed magnetism in defective graphene without presence of transition metal elements, regardless of the specific type of defects. Meanwhile, it was found that SW and DV defects would introduce small gaps in the band structures of graphene but retain the nonmagnetic behavior. In addition, the initial structural defects may be transformed into other defects by knock-off atoms, bond rotation, migration, and aggregation, which rely on the formation energies of various defects and the diffusion barriers on the transformation path. Therefore, understanding the formation and migration of defects as well as their influences on the electronic/magnetic properties of these novel 2D materials (such as graphene and silicene) not only is meaningful for fundamental research, but also provides a powerful route to tailor their physical properties and to control their functional applications in future devices. So far, many efforts have been devoted to the defects in graphene. However, to the best of our knowledge, there is no such study for the recently synthesized silicene.

In this paper, we systematically explored a variety of representative point defects in silicene sheet, including SW defect, SVs, DVs, and Si adatom. The atomic structures and their scanning tunneling microscope (STM) images were obtained by *ab initio* calculations to provide visible guidance for experimental observations. Besides, the formation energies and diffusion barriers of these defects as well as their influences on the local electronic/magnetic properties of silicene were discussed in detail. These results present primitive knowledge of defects in silicene and can give valuable information to avoid or take advantage of defects in future applications of silicene-based materials and devices.

**Simulation Methods**

*Ab initio* calculations were performed using spin polarized DFT and plane wave pseudopotential technique, as implemented in the Vienna *Ab-initio* Simulation Package (VASP). Generalized gradient approximation (GGA) with the PBE functional was adopted to describe the exchange-correlation interaction. The core electrons were described by the projected augmented wave (PAW) potentials. During all calculations, the kinetic energy cutoff of 350 eV

for the plane wave basis and the convergence criterion of  $10^{-5}$  eV for total energy were used.

Firstly, the primitive cell of silicene was fully relaxed in terms of lattice constants and atomic positions. After that, a large ( $5 \times 5$ ) supercell of silicene ( $19.45 \text{ \AA} \times 19.45 \text{ \AA}$ ) with a vacuum space of  $15 \text{ \AA}$  thickness was built to investigate the influence of various local defects. Starting from the perfect silicene sheet, the initial point defects were created by Si-Si bond rotation, removing some lattice atoms or adding extra Si atoms, respectively. For the defective silicene systems, the atomic positions were fully relaxed with fixed dimension of supercell. After geometry optimization, accurate total energies and band structures were calculated. To assess the choice of supercell size, we also chose a larger ( $7 \times 7$ ) supercell containing a DV defect. The electronic band structures of ( $5 \times 5$ ) and ( $7 \times 7$ ) silicene supercell with a DV defect are consistent with each other, implying the ( $5 \times 5$ ) supercell of silicene is sufficient to model the local defects of silicene.

To simulate the defect diffusion behavior in silicene, the climbing image nudged elastic band (cNEB) method was employed to search the diffusion path and energy barrier. During geometry optimizations and cNEB search, a ( $2 \times 2 \times 1$ )  $\mathbf{k}$ -point mesh including the  $\Gamma$  point was used to sample the reciprocal space due to the large supercell. For the calculations of energies and band structures, the  $\mathbf{k}$ -point mesh was increased to ( $6 \times 6 \times 1$ ) in order to obtain more accurate results. The force criterion for structures optimization and cNEB search was set to  $0.02 \text{ eV/\AA}$ .

## Results and discussion

To characterize the stability of a defect in silicene, we defined its formation energy  $\mathcal{E}_F$  as:

$$\mathcal{E}_F = (\mathcal{E}_T - N \times \mathcal{E}_{Si}) \quad (1)$$

where  $\mathcal{E}_T$  is the total energy of defective silicene,  $N$  is the number of silicon atoms in the supercell of defective silicene,  $\mathcal{E}_{Si}$  is the energy per silicon atom in a perfect silicene sheet.

The local structures of six typical point defects in silicene are presented in Fig. 1. Different from the planar structure of graphene, silicene possesses low buckled structure from theoretical predictions and experimental observations. As a result, various complicated superstructures of silicene on metallic surfaces were observed via STM images, which is difficult to identify. Therefore, to help recognize defects in future experiments, the STM images of these six point defects were both simulated at  $+0.5 \text{ V}$  and  $-0.5 \text{ V}$  bias, separately.

To assess the probability of formation and thermodynamic stability of these defects, their formation energies are computed and listed in Table 1, compared with the values for graphene sheet from literature. Obviously, the formation energies ( $2.09 \sim 3.77 \text{ eV}$ ) of all kinds of defects in silicene are systematically lower than those in graphene ( $4.5 \sim 8.7 \text{ eV}$ ), with exception at adatom (which is exothermic

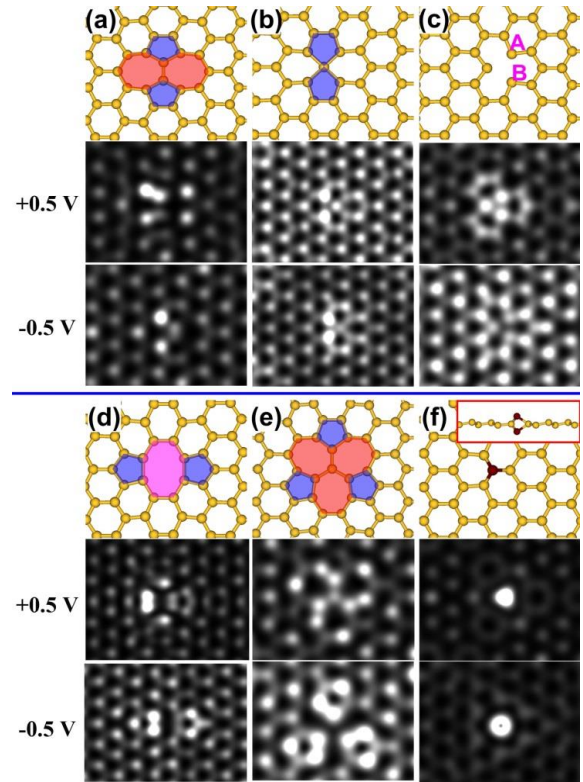


**Fig. 1** Atomic structures (upper plots) and their simulated STM images (lower plots) of silicene with various local point defects at  $\pm 0.5 \text{ V}$  bias: (a) SW; (b) SV-1 by (55|66) rings; (c) SV-2 with three dangling atoms; (d) DV-1(5|8|5); (e) reconstructed DV-2(555|777); (f) Si adatom.

for silicene but highly unfavorable for graphene). This is related to the smaller binding energy of silicene ( $\mathcal{E}_B = 3.96 \text{ eV}$  for silicene versus  $\mathcal{E}_B = 7.90 \text{ eV}$  for graphene). Thereby, under high-energy irradiations of laser, electrons and ions, the structural defects considered here, such as SW rotation, single and double vacancies would be much easily created in silicene with regard to graphene. Hence, identification those structural defects as well as understanding their migration behaviors and impacts on electronic/magnetic properties are crucial for future applications of silicene materials. At finite temperature  $T$ , the average equilibrium concentration of defects in silicene can be estimated by

$$n / N = \exp(\mathcal{E}_F / k_B T) \quad (2)$$

where  $n$  is the number of defect atom,  $N$  is number of total atoms in silicene,  $k_B$  is the Boltzmann constant. Even at a moderate temperature of  $500 \text{ K}$  (which is around the substrate temperature for silicene synthesis), Eq.(2) still yields a very low defect density. Therefore, in the ideal case at the thermodynamic limit, defect-free silicene sheet can be grown to rather large scale.

Fig. 1a presents a local SW defect formed by a Si-Si bond rotation of  $90^\circ$ , similar to those in the carbon nanotube and graphene. However, much different from easier-to-understand of STM images in graphene, the STM images of SW in silicene are rather difficult to correlate with the atomic structure. There are two local bright spots with distance of about  $4.3 \text{ \AA}$  in the STM image at  $-0.5 \text{ V}$  bias, while

five local bright spots appear in the STM image at +0.5 V bias. Note that the distribution of STM bright spots is asymmetric to the defect center, which is a direct consequence of height variation due to buckling of silicene sheet. Similar phenomena are observed in the other point defects like SV-1 (Fig. 1b), DV-1 (Fig. 1d), DV-2 (Fig. 1e).

There are two types of SVs in silicene, namely, SV-1(55|66)(Fig. 1b) and SV-2 (Fig. 1c), with distinctly different STM images. SV-1(55|66) includes a  $sp^2$ -hybridized central carbon atom and SV-2 has three dangling atoms. The distance between atom A and B is about 3.27 Å. The formation energy of a SV-1 defect is 0.76 eV lower than that of SV-2 one. Similar SV-1 structure was reported to be metastable in nanotube, but not found in infinite graphene. Interestingly, the most stable SV(5|9) defect in graphene is not preferred in silicene. It is also worthy to mention that the SV-1(55|66) may become more and more stable as the size of a finite graphene patch reduces, and even prevail the (5|9) vacancy at very small graphene quantum dots and narrow graphene ribbons according to previous calculations by Gao et al. We expect this effect should be more pronounced in finite silicene.

Fig. 1(d, e) shows two types of DV in silicene, i.e., DV-1(5|8|5) and DV-2 (555|777). The computed formation energies of them are 3.70 eV and 2.84 eV, which are 2.32 eV and 3.18 eV lower than two isolated SVs, respectively. Such remarkable energy reduction drives SVs to coalesce into DVs by diffusion. DV-1(5|8|5) is the initial structure after two SVs coalesce together, which has been extensively studied in graphene. Like the case of graphene, DV-1(5|8|5) can transform into more energetically favored DV-2(555|777) defect (0.86 eV lower in formation energy) simply through a bond rotation. The STM image of DV-1(5|8|5) have four very bright spots (Fig. 1d), implying strong localized electronic density around this defect, similar to that of graphene. But the bright zone of STM is only a half of that in graphene due to the buckling of ~0.4 Å in silicene. Interestingly, the STM image of DV-1(5|8|5) looks like that of SV-1(55|66); but the distances between two neighboring marked bright spots are about 2.5 Å for DV-1(5|8|5) and 3.4 Å for SV-1(55|66), separately. The STM image of DV-2(555|777) is easy to be distinguished at negative bias owing to the three distinct bright big rings.

Interestingly, we found that adsorption of a Si adatom on silicene sheet is exothermic with negative formation energy of -0.03 eV. As shown in Fig. 1f,

the Si adatom prefers the top site of silicene and presses down the original lattice Si atom, forming a Si<sub>2</sub> dimer with Si-Si distance of 2.7 Å embedded perpendicular to the silicene sheet. Each out-of-plane Si adatom forms three Si-Si bonds with bond angles of ~91.2°, which is somehow closer to the tetrahedron angle of 109.47° than  $sp^2$  angle of 120°. This implies that the adatom is  $sp^3$  hybridized with three neighboring Si atoms, leaving an unpaired electron on the top. This geometry is similar to Si adatom on graphene but different from C adatom on the bridge site of graphene. Another possible adsorption site for Si adatom on silicene is the hollow site, lying 0.93 eV higher than the top site. Meanwhile, the bridge site for Si adatom is unstable and moves to top site spontaneously upon relaxation. In the STM image, the adatom as a very bright spot can be easily identified, because the Si adatom is about ~1.3 Å higher than the silicene basal plane.

Owing to its high stability, particular attention should be devoted to the Si adatom. During the initial stage of silicene growth on metal surfaces, our recent study revealed considerable  $p$ - $d$  hybridization between 2D silicene clusters and Ag(111) surface,<sup>46</sup> which may suppress the adsorption of Si adatoms. However, once a Si adatom is formed, it is hard to be eliminated due to its high thermodynamic stability. Some residual Si atoms may be adsorbed on the surface of silicene after large-scale silicene were synthesized. Therefore, the influence of Si adatom needs to be carefully considered to produce high-quality silicene.

In short, the formation energies of point defects in silicene are systemically lower than graphene. The most stable SV in silicene prefers (55|66) configuration instead of the (5|9) structure in graphene, while SW and DVs have similar topological structures in both silicene and graphene. Unexpected, Si adatom on top site is energetically favored on silicene, in contrast to the high formation energy of C adatom on the bridge site of graphene.

**Table 1.** The binding energy  $\epsilon_B$  (eV) of pristine silicene and the formation energies  $\epsilon_F$  (eV) of various types of defects in silicene, comparing with the theoretical values for graphene from literature.

	$\epsilon_B$	SW	SV-1	SV-2	DV-1	DV-2	adatom
Silicene	3.96	2.09	3.01	3.77	3.70	2.84	-0.03
Graphene	7.90	4.5~5.3	7.38~7.85	-	7.52~8.7	6.4~7.5	6~7